

Search for the Standard Model Higgs Boson in the Missing Energy and Acoplanar b -Jet Topology at $\sqrt{s} = 1.96$ TeV

V. M. Abazov,³⁶ B. Abbott,⁷⁵ M. Abolins,⁶⁵ B. S. Acharya,²⁹ M. Adams,⁵¹ T. Adams,⁴⁹ E. Aguilo,⁶ M. Ahsan,⁵⁹ G. D. Alexeev,³⁶ G. Alkhazov,⁴⁰ A. Alton,^{64,*} G. Alverson,⁶³ G. A. Alves,² M. Anastasoie,³⁵ L. S. Ancu,³⁵ T. Andeen,⁵³ B. Andrieu,¹⁷ M. S. Anzels,⁵³ M. Aoki,⁵⁰ Y. Arnold,¹⁴ M. Arov,⁶⁰ M. Arthaud,¹⁸ A. Askew,⁴⁹ B. Åsman,⁴¹ A. C. S. Assis Jesus,³ O. Atramentov,⁴⁹ C. Avila,⁸ F. Badaud,¹³ L. Bagby,⁵⁰ B. Baldin,⁵⁰ D. V. Bandurin,⁵⁹ P. Banerjee,²⁹ S. Banerjee,²⁹ E. Barberis,⁶³ A.-F. Barfuss,¹⁵ P. Bargassa,⁸⁰ P. Baringer,⁵⁸ J. Barreto,² J. F. Bartlett,⁵⁰ U. Bassler,¹⁸ D. Bauer,⁴³ S. Beale,⁶ A. Bean,⁵⁸ M. Begalli,³ M. Begel,⁷³ C. Belanger-Champagne,⁴¹ L. Bellantoni,⁵⁰ A. Bellavance,⁵⁰ J. A. Benitez,⁶⁵ S. B. Beri,²⁷ G. Bernardi,¹⁷ R. Bernhard,²³ I. Bertram,⁴² M. Besançon,¹⁸ R. Beuselinck,⁴³ V. A. Bezzubov,³⁹ P. C. Bhat,⁵⁰ V. Bhatnagar,²⁷ C. Biscarat,²⁰ G. Blazey,⁵² F. Blekman,⁴³ S. Blessing,⁴⁹ K. Bloom,⁶⁷ A. Boehnlein,⁵⁰ D. Boline,⁶² T. A. Bolton,⁵⁹ E. E. Boos,³⁸ G. Borissov,⁴² T. Bose,⁷⁷ A. Brandt,⁷⁸ R. Brock,⁶⁵ G. Brooijmans,⁷⁰ A. Bross,⁵⁰ D. Brown,⁸¹ X. B. Bu,⁷ N. J. Buchanan,⁴⁹ D. Buchholz,⁵³ M. Buehler,⁸¹ V. Buescher,²² V. Bunichev,³⁸ S. Burdin,^{42,†} T. H. Burnett,⁸² C. P. Buszello,⁴³ J. M. Butler,⁶² P. Calfayan,²⁵ S. Calvet,¹⁶ J. Cammin,⁷¹ E. Carrera,⁴⁹ W. Carvalho,³ B. C. K. Casey,⁵⁰ H. Castilla-Valdez,³³ S. Chakrabarti,¹⁸ D. Chakraborty,⁵² K. M. Chan,⁵⁵ A. Chandra,⁴⁸ E. Cheu,⁴⁵ F. Chevallier,¹⁴ D. K. Cho,⁶² S. Choi,³² B. Choudhary,²⁸ L. Christofek,⁷⁷ T. Christoudias,⁴³ S. Cihangir,⁵⁰ D. Claes,⁶⁷ J. Clutter,⁵⁸ M. Cooke,⁵⁰ W. E. Cooper,⁵⁰ M. Corcoran,⁸⁰ F. Couderc,¹⁸ M.-C. Cousinou,¹⁵ S. Crépe-Renaudin,¹⁴ V. Cuplov,⁵⁹ D. Cutts,⁷⁷ M. Cwiok,³⁰ H. da Motta,² A. Das,⁴⁵ G. Davies,⁴³ K. De,⁷⁸ S. J. de Jong,³⁵ E. De La Cruz-Burelo,³³ C. De Oliveira Martins,³ K. DeVaughan,⁶⁷ J. D. Degenhardt,⁶⁴ F. Déliot,¹⁸ M. Demarteau,⁵⁰ R. Demina,⁷¹ D. Denisov,⁵⁰ S. P. Denisov,³⁹ S. Desai,⁵⁰ H. T. Diehl,⁵⁰ M. Diesburg,⁵⁰ A. Dominguez,⁶⁷ H. Dong,⁷² T. Dorland,⁸² A. Dubey,²⁸ L. V. Dudko,³⁸ L. Dufлот,¹⁶ S. R. Dugad,²⁹ D. Duggan,⁴⁹ A. Duperrin,¹⁵ J. Dyer,⁶⁵ A. Dyshkant,⁵² M. Eads,⁶⁷ D. Edmunds,⁶⁵ J. Ellison,⁴⁸ V. D. Elvira,⁵⁰ Y. Enari,⁷⁷ S. Eno,⁶¹ P. Ermolov,^{38,††} H. Evans,⁵⁴ A. Evdokimov,⁷³ V. N. Evdokimov,³⁹ A. V. Ferapontov,⁵⁹ T. Ferbel,⁷¹ F. Fiedler,²⁴ F. Filthaut,³⁵ W. Fisher,⁵⁰ H. E. Fisk,⁵⁰ M. Fortner,⁵² H. Fox,⁴² S. Fu,⁵⁰ S. Fuess,⁵⁰ T. Gadfort,⁷⁰ C. F. Galea,³⁵ C. Garcia,⁷¹ A. Garcia-Bellido,⁷¹ V. Gavrilov,³⁷ P. Gay,¹³ W. Geist,¹⁹ W. Geng,^{15,65} C. E. Gerber,⁵¹ Y. Gershtein,⁴⁹ D. Gillberg,⁶ G. Ginther,⁷¹ N. Gollub,⁴¹ B. Gómez,⁸ A. Goussiou,⁸² P. D. Grannis,⁷² H. Greenlee,⁵⁰ Z. D. Greenwood,⁶⁰ E. M. Gregores,⁴ G. Grenier,²⁰ Ph. Gris,¹³ J.-F. Grivaz,¹⁶ A. Grohsjean,²⁵ S. Grünendahl,⁵⁰ M. W. Grünewald,³⁰ F. Guo,⁷² J. Guo,⁷² G. Gutierrez,⁵⁰ P. Gutierrez,⁷⁵ A. Haas,⁷⁰ N. J. Hadley,⁶¹ P. Haefner,²⁵ S. Hagopian,⁴⁹ J. Haley,⁶⁸ I. Hall,⁶⁵ R. E. Hall,⁴⁷ L. Han,⁷ K. Harder,⁴⁴ A. Harel,⁷¹ J. M. Hauptman,⁵⁷ J. Hays,⁴³ T. Hebbeker,²¹ D. Hedin,⁵² J. G. Hegeman,³⁴ A. P. Heinson,⁴⁸ U. Heintz,⁶² C. Hensel,^{22,§} K. Herner,⁷² G. Hesketh,⁶³ M. D. Hildreth,⁵⁵ R. Hirosky,⁸¹ J. D. Hobbs,⁷² B. Hoeneisen,¹² H. Hoeth,²⁶ M. Hohlfeld,²² S. Hossain,⁷⁵ P. Houben,³⁴ Y. Hu,⁷² Z. Hubacek,¹⁰ V. Hynek,⁹ I. Iashvili,⁶⁹ R. Illingworth,⁵⁰ A. S. Ito,⁵⁰ S. Jabeen,⁶² M. Jaffré,¹⁶ S. Jain,⁷⁵ K. Jakobs,²³ C. Jarvis,⁶¹ R. Jesik,⁴³ K. Johns,⁴⁵ C. Johnson,⁷⁰ M. Johnson,⁵⁰ D. Johnston,⁶⁷ A. Jonckheere,⁵⁰ P. Jonsson,⁴³ A. Juste,⁵⁰ E. Kajfasz,¹⁵ J. M. Kalk,⁶⁰ D. Karmanov,³⁸ P. A. Kasper,⁵⁰ I. Katsanos,⁷⁰ D. Kau,⁴⁹ V. Kaushik,⁷⁸ R. Kehoe,⁷⁹ S. Kermiche,¹⁵ N. Khalatyan,⁵⁰ A. Khanov,⁷⁶ A. Kharchilava,⁶⁹ Y. M. Kharzheev,³⁶ D. Khatidze,⁷⁰ T. J. Kim,³¹ M. H. Kirby,⁵³ M. Kirsch,²¹ B. Klima,⁵⁰ J. M. Kohli,²⁷ J.-P. Konrath,²³ A. V. Kozelov,³⁹ J. Kraus,⁶⁵ T. Kuhl,²⁴ A. Kumar,⁶⁹ A. Kupco,¹¹ T. Kurča,²⁰ V. A. Kuzmin,³⁸ J. Kvita,⁹ F. Lacroix,¹³ D. Lam,⁵⁵ S. Lammers,⁷⁰ G. Landsberg,⁷⁷ P. Lebrun,²⁰ W. M. Lee,⁵⁰ A. Leflat,³⁸ J. Lellouch,¹⁷ J. Li,^{78,††} L. Li,⁴⁸ Q. Z. Li,⁵⁰ S. M. Lietti,⁵ J. K. Lim,³¹ J. G. R. Lima,⁵² D. Lincoln,⁵⁰ J. Linnemann,⁶⁵ V. V. Lipaev,³⁹ R. Lipton,⁵⁰ Y. Liu,⁷ Z. Liu,⁶ A. Lobodenko,⁴⁰ M. Lokajicek,¹¹ P. Love,⁴² H. J. Lubatti,⁸² R. Luna,³ A. L. Lyon,⁵⁰ A. K. A. Maciel,² D. Mackin,⁸⁰ R. J. Madaras,⁴⁶ P. Mättig,²⁶ C. Magass,²¹ A. Magerkurth,⁶⁴ P. K. Mal,⁸² H. B. Malbouisson,³ S. Malik,⁶⁷ V. L. Malyshev,³⁶ Y. Maravin,⁵⁹ B. Martin,¹⁴ R. McCarthy,⁷² A. Melnitchouk,⁶⁶ L. Mendoza,⁸ P. G. Mercadante,⁵ M. Merkin,³⁸ K. W. Merritt,⁵⁰ A. Meyer,²¹ J. Meyer,^{22,§} J. Mitrevski,⁷⁰ R. K. Mommsen,⁴⁴ N. K. Mondal,²⁹ R. W. Moore,⁶ T. Moulik,⁵⁸ G. S. Muanza,²⁰ M. Mulhearn,⁷⁰ O. Mundal,²² L. Mundim,³ E. Nagy,¹⁵ M. Naimuddin,⁵⁰ M. Narain,⁷⁷ N. A. Naumann,³⁵ H. A. Neal,⁶⁴ J. P. Negret,⁸ P. Neustroev,⁴⁰ H. Nilsen,²³ H. Nogima,³ S. F. Novaes,⁵ T. Nunnemann,²⁵ V. O'Dell,⁵⁰ D. C. O'Neil,⁶ G. Obrant,⁴⁰ C. Ochando,¹⁶ D. Onoprienko,⁵⁹ N. Oshima,⁵⁰ N. Osman,⁴³ J. Osta,⁵⁵ R. Otec,¹⁰ G. J. Otero y Garzón,⁵⁰ M. Owen,⁴⁴ P. Padley,⁸⁰ M. Pangilinan,⁷⁷ N. Parashar,⁵⁶ S.-J. Park,^{22,§} S. K. Park,³¹ J. Parsons,⁷⁰ R. Partridge,⁷⁷ N. Parua,⁵⁴ A. Patwa,⁷³ G. Pawloski,⁸⁰ B. Penning,²³ M. Perfilov,³⁸ K. Peters,⁴⁴ Y. Peters,²⁶ P. Pétröff,¹⁶ M. Petteni,⁴³ R. Piegaia,¹ J. Piper,⁶⁵ M.-A. Pleier,²² P. L. M. Podesta-Lerma,^{33,‡} V. M. Podstavkov,⁵⁰ Y. Pogorelov,⁵⁵ M.-E. Pol,² P. Polozov,³⁷ B. G. Pope,⁶⁵ A. V. Popov,³⁹ C. Potter,⁶ W. L. Prado da Silva,³ H. B. Prosper,⁴⁹ S. Protopopescu,⁷³ J. Qian,⁶⁴ A. Quadt,^{22,§} B. Quinn,⁶⁶ A. Rakitine,⁴² M. S. Rangel,² K. Ranjan,²⁸ P. N. Ratoff,⁴² P. Renkel,⁷⁹ P. Rich,⁴⁴

J. Rieger,⁵⁴ M. Rijssenbeek,⁷² I. Ripp-Baudot,¹⁹ F. Rizatdinova,⁷⁶ S. Robinson,⁴³ R. F. Rodrigues,³ M. Rominsky,⁷⁵ C. Royon,¹⁸ P. Rubinov,⁵⁰ R. Ruchti,⁵⁵ G. Safronov,³⁷ G. Sajot,¹⁴ A. Sánchez-Hernández,³³ M. P. Sanders,¹⁷ B. Sanghi,⁵⁰ G. Savage,⁵⁰ L. Sawyer,⁶⁰ T. Scanlon,⁴³ D. Schaile,²⁵ R. D. Schamberger,⁷² Y. Scheglov,⁴⁰ H. Schellman,⁵³ T. Schliephake,²⁶ S. Schlobohm,⁸² C. Schwanenberger,⁴⁴ A. Schwartzman,⁶⁸ R. Schwienhorst,⁶⁵ J. Sekaric,⁴⁹ H. Severini,⁷⁵ E. Shabalina,⁵¹ M. Shamim,⁵⁹ V. Shary,¹⁸ A. A. Shchukin,³⁹ R. K. Shivpuri,²⁸ V. Siccaldi,¹⁹ V. Simak,¹⁰ V. Sirotenko,⁵⁰ P. Skubic,⁷⁵ P. Slattery,⁷¹ D. Smirnov,⁵⁵ G. R. Snow,⁶⁷ J. Snow,⁷⁴ S. Snyder,⁷³ S. Söldner-Rembold,⁴⁴ L. Sonnenschein,¹⁷ A. Sopczak,⁴² M. Sosebee,⁷⁸ K. Soustruznik,⁹ B. Spurlock,⁷⁸ J. Stark,¹⁴ J. Steele,⁶⁰ V. Stolin,³⁷ D. A. Stoyanova,³⁹ J. Strandberg,⁶⁴ S. Strandberg,⁴¹ M. A. Strang,⁶⁹ E. Strauss,⁷² M. Strauss,⁷⁵ R. Ströhmer,²⁵ D. Strom,⁵³ L. Stutte,⁵⁰ S. Sumowidagdo,⁴⁹ P. Svoisky,⁵⁵ A. Sznajder,³ P. Tamburello,⁴⁵ A. Tanasijczuk,¹ W. Taylor,⁶ B. Tiller,²⁵ F. Tissandier,¹³ M. Titov,¹⁸ V. V. Tokmenin,³⁶ I. Torchiani,²³ D. Tsybychev,⁷² B. Tuchming,¹⁸ C. Tully,⁶⁸ P. M. Tuts,⁷⁰ R. Unalan,⁶⁵ L. Uvarov,⁴⁰ S. Uvarov,⁴⁰ S. Uzunyan,⁵² B. Vachon,⁶ P. J. van den Berg,³⁴ R. Van Kooten,⁵⁴ W. M. van Leeuwen,³⁴ N. Varelas,⁵¹ E. W. Varnes,⁴⁵ I. A. Vasilyev,³⁹ P. Verdier,²⁰ L. S. Vertogradov,³⁶ M. Verzocchi,⁵⁰ D. Vilanova,¹⁸ F. Villeneuve-Seguirer,⁴³ P. Vint,⁴³ P. Vokac,¹⁰ M. Voutilainen,^{67,||} R. Wagner,⁶⁸ H. D. Wahl,⁴⁹ M. H. L. S. Wang,⁵⁰ J. Warchol,⁵⁵ G. Watts,⁸² M. Wayne,⁵⁵ G. Weber,²⁴ M. Weber,^{50,||} L. Welty-Rieger,⁵⁴ A. Wenger,^{23,**} N. Wermes,²² M. Wetstein,⁶¹ A. White,⁷⁸ D. Wicke,²⁶ M. Williams,⁴² G. W. Wilson,⁵⁸ S. J. Wimpenny,⁴⁸ M. Wobisch,⁶⁰ D. R. Wood,⁶³ T. R. Wyatt,⁴⁴ Y. Xie,⁷⁷ S. Yacoub,⁵³ R. Yamada,⁵⁰ W.-C. Yang,⁴⁴ T. Yasuda,⁵⁰ Y. A. Yatsunenko,³⁶ H. Yin,⁷ K. Yip,⁷³ H. D. Yoo,⁷⁷ S. W. Youn,⁵³ J. Yu,⁷⁸ C. Zeitnitz,²⁶ S. Zelitch,⁸¹ T. Zhao,⁸² B. Zhou,⁶⁴ J. Zhu,⁷² M. Zielinski,⁷¹ D. Zieminska,⁵⁴ A. Zieminski,^{54,††} L. Zivkovic,⁷⁰ V. Zutshi,⁵² and E. G. Zverev³⁸

(D0 Collaboration)

¹Universidad de Buenos Aires, Buenos Aires, Argentina²LAFEX, Centro Brasileiro de Pesquisas Físicas, Rio de Janeiro, Brazil³Universidade do Estado do Rio de Janeiro, Rio de Janeiro, Brazil⁴Universidade Federal do ABC, Santo André, Brazil⁵Instituto de Física Teórica, Universidade Estadual Paulista, São Paulo, Brazil⁶University of Alberta, Edmonton, Alberta, Canada,

Simon Fraser University, Burnaby, British Columbia, Canada,

York University, Toronto, Ontario, Canada,

and McGill University, Montreal, Quebec, Canada

⁷University of Science and Technology of China, Hefei, People's Republic of China⁸Universidad de los Andes, Bogotá, Colombia⁹Center for Particle Physics, Charles University, Prague, Czech Republic¹⁰Czech Technical University, Prague, Czech Republic¹¹Center for Particle Physics, Institute of Physics, Academy of Sciences of the Czech Republic, Prague, Czech Republic¹²Universidad San Francisco de Quito, Quito, Ecuador¹³LPC, Université Blaise Pascal, CNRS/IN2P3, Clermont, France¹⁴LPSC, Université Joseph Fourier Grenoble 1, CNRS/IN2P3, Institut National Polytechnique de Grenoble, Grenoble, France¹⁵CPPM, Aix-Marseille Université, CNRS/IN2P3, Marseille, France¹⁶LAL, Université Paris-Sud, IN2P3/CNRS, Orsay, France¹⁷LPNHE, IN2P3/CNRS, Universités Paris VI and VII, Paris, France¹⁸CEA, Ifju, SPP, Saclay, France¹⁹IPHC, Université Louis Pasteur, CNRS/IN2P3, Strasbourg, France²⁰IPNL, Université Lyon 1, CNRS/IN2P3, Villeurbanne, France and Université de Lyon, Lyon, France²¹III. Physikalisches Institut A, RWTH Aachen University, Aachen, Germany²²Physikalisches Institut, Universität Bonn, Bonn, Germany²³Physikalisches Institut, Universität Freiburg, Freiburg, Germany²⁴Institut für Physik, Universität Mainz, Mainz, Germany²⁵Ludwig-Maximilians-Universität München, München, Germany²⁶Fachbereich Physik, University of Wuppertal, Wuppertal, Germany²⁷Panjab University, Chandigarh, India²⁸Delhi University, Delhi, India²⁹Tata Institute of Fundamental Research, Mumbai, India³⁰University College Dublin, Dublin, Ireland³¹Korea Detector Laboratory, Korea University, Seoul, Korea³²SungKyunKwan University, Suwon, Korea³³CINVESTAV, Mexico City, Mexico

- ³⁴FOM-Institute NIKHEF and University of Amsterdam/NIKHEF, Amsterdam, The Netherlands
³⁵Radboud University Nijmegen/NIKHEF, Nijmegen, The Netherlands
³⁶Joint Institute for Nuclear Research, Dubna, Russia
³⁷Institute for Theoretical and Experimental Physics, Moscow, Russia
³⁸Moscow State University, Moscow, Russia
³⁹Institute for High Energy Physics, Protvino, Russia
⁴⁰Petersburg Nuclear Physics Institute, St. Petersburg, Russia
⁴¹Lund University, Lund, Sweden, Royal Institute of Technology and Stockholm University, Stockholm, Sweden, and Uppsala University, Uppsala, Sweden
⁴²Lancaster University, Lancaster, United Kingdom
⁴³Imperial College, London, United Kingdom
⁴⁴University of Manchester, Manchester, United Kingdom
⁴⁵University of Arizona, Tucson, Arizona 85721, USA
⁴⁶Lawrence Berkeley National Laboratory and University of California, Berkeley, California 94720, USA
⁴⁷California State University, Fresno, California 93740, USA
⁴⁸University of California, Riverside, California 92521, USA
⁴⁹Florida State University, Tallahassee, Florida 32306, USA
⁵⁰Fermi National Accelerator Laboratory, Batavia, Illinois 60510, USA
⁵¹University of Illinois at Chicago, Chicago, Illinois 60607, USA
⁵²Northern Illinois University, DeKalb, Illinois 60115, USA
⁵³Northwestern University, Evanston, Illinois 60208, USA
⁵⁴Indiana University, Bloomington, Indiana 47405, USA
⁵⁵University of Notre Dame, Notre Dame, Indiana 46556, USA
⁵⁶Purdue University Calumet, Hammond, Indiana 46323, USA
⁵⁷Iowa State University, Ames, Iowa 50011, USA
⁵⁸University of Kansas, Lawrence, Kansas 66045, USA
⁵⁹Kansas State University, Manhattan, Kansas 66506, USA
⁶⁰Louisiana Tech University, Ruston, Louisiana 71272, USA
⁶¹University of Maryland, College Park, Maryland 20742, USA
⁶²Boston University, Boston, Massachusetts 02215, USA
⁶³Northeastern University, Boston, Massachusetts 02115, USA
⁶⁴University of Michigan, Ann Arbor, Michigan 48109, USA
⁶⁵Michigan State University, East Lansing, Michigan 48824, USA
⁶⁶University of Mississippi, University, Mississippi 38677, USA
⁶⁷University of Nebraska, Lincoln, Nebraska 68588, USA
⁶⁸Princeton University, Princeton, New Jersey 08544, USA
⁶⁹State University of New York, Buffalo, New York 14260, USA
⁷⁰Columbia University, New York, New York 10027, USA
⁷¹University of Rochester, Rochester, New York 14627, USA
⁷²State University of New York, Stony Brook, New York 11794, USA
⁷³Brookhaven National Laboratory, Upton, New York 11973, USA
⁷⁴Langston University, Langston, Oklahoma 73050, USA
⁷⁵University of Oklahoma, Norman, Oklahoma 73019, USA
⁷⁶Oklahoma State University, Stillwater, Oklahoma 74078, USA
⁷⁷Brown University, Providence, Rhode Island 02912, USA
⁷⁸University of Texas, Arlington, Texas 76019, USA
⁷⁹Southern Methodist University, Dallas, Texas 75275, USA
⁸⁰Rice University, Houston, Texas 77005, USA
⁸¹University of Virginia, Charlottesville, Virginia 22901, USA
⁸²University of Washington, Seattle, Washington 98195, USA
(Received 15 August 2008; published 17 December 2008)

We report a search for the standard model Higgs boson in the missing energy and acoplanar b -jet topology, using an integrated luminosity of 0.93 fb^{-1} recorded by the D0 detector at the Fermilab Tevatron $p\bar{p}$ Collider. The analysis includes signal contributions from $p\bar{p} \rightarrow ZH \rightarrow \nu\bar{\nu}b\bar{b}$, as well as from WH production in which the charged lepton from the W boson decay is undetected. Neural networks are used to separate signal from background. In the absence of a signal, we set limits on $\sigma(p\bar{p} \rightarrow VH) \times B(H \rightarrow b\bar{b})$ at the 95% C.L. of 2.6–2.3 pb, for Higgs boson masses in the range 105–135 GeV, where $V = W, Z$. The corresponding expected limits range from 2.8 to 2.0 pb.

The Higgs mechanism, postulated to explain electroweak symmetry breaking, predicts the existence of the Higgs boson, which has yet to be found. The CERN LEP e^+e^- Collider experiments placed a lower limit on its mass of 114.4 GeV at 95% C.L. [1]. Global fits to precision electroweak data suggest a mass of $M_H < 185$ GeV at 95% C.L. when combined with the direct searches [2]. In this range, the Fermilab Tevatron $p\bar{p}$ Collider has significant discovery potential. Searches in the missing energy and acoplanar b -jet channel have been published by CDF [3] and D0 [4]. This channel is sensitive to ZH associated production when the Z decays to neutrinos and WH production when the charged lepton from the W decay is undetected. It is complementary to searches with visible leptons in the final state [5–8] and contributes significantly to the discovery potential of a low mass Higgs boson. At the Tevatron it provides the best sensitivity along with the search for $WH \rightarrow \ell\nu_\ell b\bar{b}$. The result in this Letter supersedes our previous work. As well as benefitting from more data, this analysis is enhanced through the use of artificial neural networks (NN) for heavy flavor tagging (b tagging) and in event selection.

The D0 detector is described in Ref. [9]. Dedicated triggers selected events with acoplanar jets and large imbalance in transverse momentum, (\cancel{E}_T), as defined by energy deposited in the D0 calorimeters. After imposing data quality requirements the data correspond to an integrated luminosity of 0.93 fb^{-1} [10]. Time-dependent adjustments have been made to the trigger requirements to compensate for the increasing peak instantaneous luminosity of the Tevatron. The selection criteria therefore varied somewhat, but typical requirements using jets reconstructed at the highest level trigger [9] were $\cancel{H}_T > 30$ GeV, where \cancel{H}_T is the imbalance in transverse momentum from jets, and an azimuthal angle between the two leading (highest p_T) jets of $\Delta\phi(\text{jet}_1, \text{jet}_2) < 170^\circ$.

Event selection requires at least two jets with $p_T > 20$ GeV, $|\eta| < 1.1$ (central calorimeter) or $1.4 < |\eta| < 2.5$ (end calorimeters) and $\Delta\phi(\text{jet}_1, \text{jet}_2) < 165^\circ$, where η is the pseudorapidity measured from the center of the detector. Reconstructed jets are corrected based on the expected calorimeter response, energy lost due to showering out of the jet cone, and energy deposited in the jet cone not associated with the jet [11]. We require the distance along the beam axis of the primary vertex from the center of the detector (z_{PV}) to be less than 35 cm, and at least three tracks attached to the primary vertex to ensure b tagging capability. In order to reduce the contribution from $t\bar{t}$ background, we also require $\cancel{E}_T > 50$ GeV and $H_T < 240$ GeV, where H_T is the scalar sum of the transverse momenta of selected jets. A significant proportion of W/Z + jets events in which the bosons decay into charged leptons are rejected by vetoing isolated leptons (electrons or muons).

Signal samples of $ZH \rightarrow \nu\nu b\bar{b}$ and $WH \rightarrow \ell\nu_\ell b\bar{b}$ ($\ell = e, \mu, \tau$) were generated for $105 \leq M_H \leq 135$ GeV in 10 GeV increments using PYTHIA [12]. There are two types of backgrounds: physical processes modeled by Monte Carlo (MC) generators and instrumental background predicted from data. ALPGEN [13] was used to simulate $t\bar{t}$ production with up to four jets. Samples of W + jets (W decays to all three lepton pairs for light jets $jj, b\bar{b}$ and $c\bar{c}$ jets) and Z + jets (including $Z \rightarrow \nu\bar{\nu}$ and $Z \rightarrow \tau^+\tau^-$ processes for $jj, b\bar{b}$ and $c\bar{c}$ jets) were also generated separately using ALPGEN. Diboson processes (WW, WZ and ZZ) were generated with PYTHIA. The samples generated with ALPGEN were processed through PYTHIA for showering and hadronization. Next-to-leading order (NLO) cross sections were used for normalizing all processes (NNLO for $t\bar{t}$). All samples were processed through the GEANT3-based D0 detector simulation [14] and the reconstruction software. The trigger requirements were modeled using a parametrized trigger simulation determined from data.

As b tagging is applied later, jets are required to be “taggable”, i.e., satisfy certain minimal tracking and vertexing criteria; a jet must have at least two tracks, one with $p_T > 1$ and the other with > 0.5 GeV, each with ≥ 2 hits in the silicon vertex detector, and $\Delta\mathcal{R}(\text{track}, \text{jet}) < 0.5$, where $\Delta\mathcal{R} = \sqrt{(\Delta\phi)^2 + (\Delta\eta)^2}$, with ϕ being the azimuthal angle. The fraction of taggable jets was investigated as a function of p_T, η and z_{PV} using a W + jets data sample. The taggability of simulated jets is corrected by the ratio of taggabilities measured in data and MC samples, which is found to depend only on η . Correction factors of 0.97 ± 0.01 and 0.95 ± 0.03 (statistical errors) are used for the central and end calorimeters, respectively.

For events originating from hard processes with genuine missing transverse energy, the $\cancel{H}_T, \cancel{E}_T$ and \cancel{T}_T (where \cancel{T}_T is

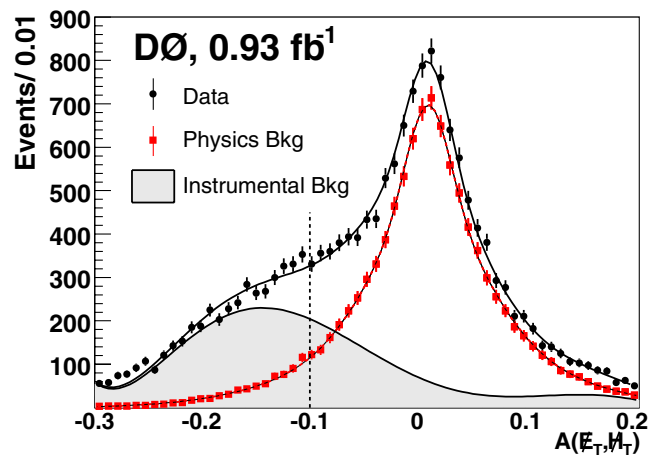


FIG. 1 (color online). $\mathcal{A}(\cancel{E}_T, \cancel{H}_T)$ for data, MC physics background and instrumental background in the signal region, before implementing b tagging. The final selection corresponds to $-0.1 < \mathcal{A}(\cancel{E}_T, \cancel{H}_T) < 0.2$.

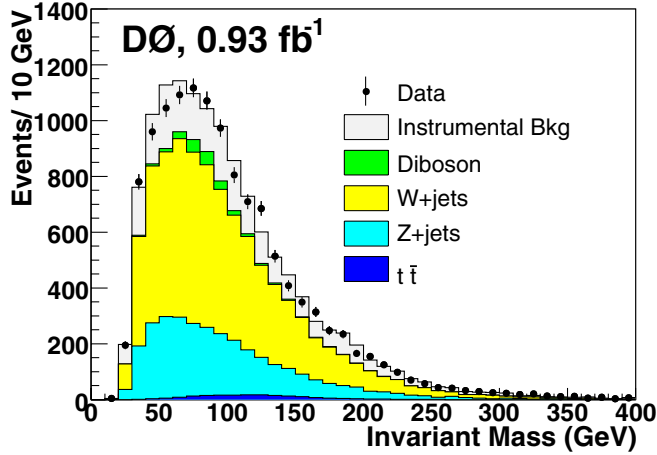


FIG. 2 (color online). Invariant mass distribution of the two leading jets before b tagging requirements.

the negative of the vector sum of the p_T of all tracks) point in the same direction and are correlated. However, dijet events in which one of the jets has been mismeasured typically have \cancel{E}_T pointing along the direction of one of the jets. Instrumental effects produce events that tend to have \cancel{E}_T and \cancel{T}_T misaligned. To reduce instrumental background, we require: (i) $\min\{\Delta\phi_i(\cancel{E}_T, \text{jet}_i)\} > 0.15$, where $\min\{\Delta\phi_i(\cancel{E}_T, \text{jet}_i)\}$ is the minimum of the difference in azimuthal angle between the direction of \cancel{E}_T and any of the jets; (ii) $\cancel{E}_T(\text{GeV}) > -40 \times \min\{\Delta\phi_i(\cancel{E}_T, \text{jet}_i)\} + 80$; (iii) $\Delta\phi(\cancel{E}_T, \cancel{T}_T) < \pi/2$, where $\Delta\phi(\cancel{E}_T, \cancel{T}_T)$ is the difference in azimuthal angle between the directions of \cancel{E}_T and \cancel{T}_T ; (iv) $-0.1 < \mathcal{A}(\cancel{E}_T, \cancel{H}_T) < 0.2$, where $\mathcal{A}(\cancel{E}_T, \cancel{H}_T) \equiv (\cancel{E}_T - \cancel{H}_T)/(\cancel{E}_T + \cancel{H}_T)$ is the asymmetry between \cancel{E}_T and \cancel{H}_T .

The residual contribution of the instrumental background is determined from distributions in $\mathcal{A}(\cancel{E}_T, \cancel{H}_T)$ and $\Delta\phi(\cancel{E}_T, \cancel{T}_T)$. The instrumental background peaks at $\mathcal{A}(\cancel{E}_T, \cancel{H}_T) < 0$ because it is dominated by poor quality jets that are taken into account when calculating \cancel{E}_T but not \cancel{H}_T . Signal and sideband regions are defined as having $\Delta\phi(\cancel{E}_T, \cancel{T}_T) < \pi/2$ and $\Delta\phi(\cancel{E}_T, \cancel{T}_T) > \pi/2$, respectively. The shape of the backgrounds from simulated processes, for both regions, are taken directly from the MC calculations. We fit a sixth-order polynomial to the $\mathcal{A}(\cancel{E}_T, \cancel{H}_T)$ distribution in the sideband region to determine the shape (before b -jet tagging) for the instrumental background (after subtracting the MC background contribution) and a triple Gaussian for the signal region. We then do a combined physics and instrumental backgrounds fit to data in the signal region, as shown in Fig. 1. For this combined fit, the simulation and instrumental background shapes are fixed to those from previous fits, and only the absolute scale of the two types of background is allowed to float. The normalization of the background for simulated (MC) processes is found to be 1.06 ± 0.02 (statistical error), in good agreement with the expected cross sections. The

TABLE I. Number of events after selections.

Sample	No b -tag	Double b -tag
$ZH(M_H = 115 \text{ GeV})$	2.46 ± 0.34	0.88 ± 0.12
$WH(M_H = 115 \text{ GeV})$	1.75 ± 0.25	0.61 ± 0.08
Wjj	5180 ± 670	7.6 ± 1.4
$Wb\bar{b}$	397 ± 52	35.4 ± 7.1
$Wc\bar{c}$	1170 ± 150	9.3 ± 1.9
$Z(\rightarrow \tau^+ \tau^-)jj$	107 ± 14	0.25 ± 0.05
$Z(\rightarrow \nu\bar{\nu})jj$	2130 ± 280	0.63 ± 0.12
$Z(\rightarrow \tau^+ \tau^-)b\bar{b}$	6.39 ± 0.83	0.63 ± 0.13
$Z(\rightarrow \nu\bar{\nu})b\bar{b}$	229 ± 30	24.9 ± 5.0
$Z(\rightarrow \tau^+ \tau^-)c\bar{c}$	12.8 ± 1.7	0.18 ± 0.04
$Z(\rightarrow \nu\bar{\nu})c\bar{c}$	467 ± 61	4.9 ± 1.0
$t\bar{t}$	172 ± 34	29.1 ± 6.1
Diboson	228 ± 25	3.84 ± 0.50
Total MC Bkg	10100 ± 750	117 ± 17
Instrumental Bkg	2560 ± 330	17.2 ± 3.4
Total Bkg	12700 ± 800	134 ± 18
Observed Events	12500	140

invariant mass distribution of the two leading jets after final background normalization is shown in Fig. 2.

The standard D0 neural network b tagging algorithm employs lifetime based information involving track impact parameters and secondary vertices [15]. We optimize the choice of b tagging operating points for best signal significance and require one tight b -tag (b -tag efficiency $\sim 50\%$ for a mistag rate of $\sim 0.4\%$) and one loose b -tag (b -tag efficiency $\sim 70\%$ for a mistag rate of $\sim 4.5\%$). Table I shows the number of expected events from MC and instrumental backgrounds along with the number of events observed in data, before and after b tagging. After b tagging, 134 ± 18 events are expected and 140 are observed.

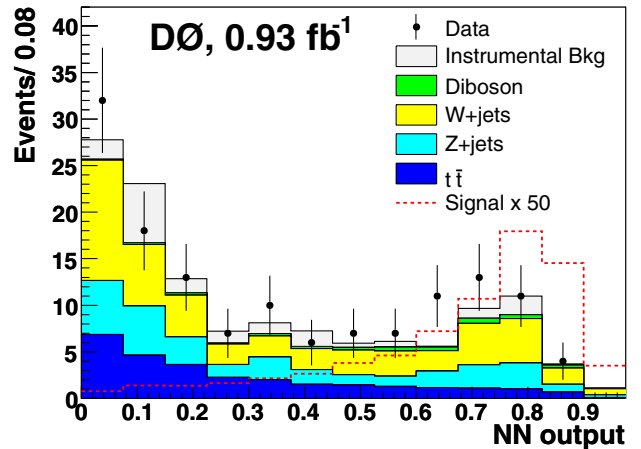


FIG. 3 (color online). NN output distributions for $M_H = 115 \text{ GeV}$ after b tagging. The MC expectation for the Higgs signal is scaled up by a factor of 50.

TABLE II. Expected (Exp.) and observed (Obs.) limits in pb and as a ratio to the SM Higgs cross section (in parentheses), assuming $H \rightarrow b\bar{b}$.

Higgs Mass (GeV)	105	115	125	135
ZH Exp.	1.6 (15)	1.5 (19)	1.4 (29)	1.2 (47)
ZH Obs.	1.5 (14)	1.5 (20)	1.4 (30)	1.3 (51)
WH Exp.	4.8 (25)	4.3 (33)	3.8 (47)	3.6 (84)
WH Obs.	4.4 (23)	5.0 (39)	4.4 (55)	4.2 (99)
VH Exp.	2.8 (9.1)	2.5 (12)	2.3 (18)	2.0 (30)
VH Obs.	2.6 (8.7)	2.7 (13)	2.5 (20)	2.3 (34)

Further signal-to-background discrimination is achieved by combining several kinematic variables using a NN. Independent MC samples are used for NN training, NN testing and limit setting. The instrumental background contribution is not taken into account during training, as its inclusion does not improve the expected sensitivity. The signal sample used for training is a combination of the ZH and WH contributions, weighted such that the total contribution from each sample is that expected after b tagging. The NN input variables are the invariant mass of the two leading jets in the event, $\Delta\mathcal{R}$ between the two jets, p_T of the leading jet, p_T of the next-to-leading jet, \cancel{E}_T , \cancel{H}_T and H_T . The input variables are selected for their ability to separate signal and background and to provide good modeling of data. The NN outputs for signal, background and data are shown in Fig. 3.

Systematic uncertainties affect the expected number of signal and background events (“overall uncertainties”) as well as the shape of the distribution in the NN output (“differential uncertainties”). We estimate overall systematic uncertainties associated with luminosity (6.1%), trigger efficiencies (5%), jet identification (5%), b tagging (7%), background MC cross section (6%–18%) and instrumental background (20%). All systematic uncertainties are common and correlated between signal and backgrounds, except for the uncertainties on the cross sections and the instrumental background. Differential uncertainties are estimated from the difference in the shape of the NN output by varying the jet energy scale (JES) by its uncertainties in a correlated way for all signal and background MC samples at each mass point. The difference in the distribution of the NN output from the uncertainty in the shape of the MC di- b -jet mass spectrum associated with the parameters of the generator is also taken into account at each M_H point. The JES uncertainty was estimated to be $\leq 10\%$ and that for the mass spectrum $\leq 8\%$. Additionally, the impact on the NN output of the discrepancy in the low mass region in Fig. 2 was investigated and found to be negligible.

In the absence of any significant enhancement we set a limit on the Higgs production cross section using a modified frequentist approach with a Poisson log-likelihood ratio (LLR) statistic [16,17]. The NN distribution is used to construct the LLR test statistic. The impact of systematic

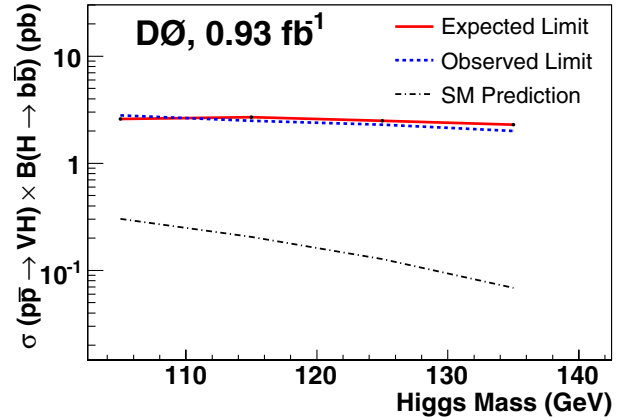


FIG. 4 (color online). 95% C.L. upper limit on $\sigma(p\bar{p} \rightarrow VH) \times B(H \rightarrow b\bar{b})$ (and corresponding expected limit) for VH production versus Higgs boson mass.

uncertainties is incorporated through “marginalization” of the Poisson probability distributions for signal and background, assuming Gaussian distributions. We adjust each component of systematic uncertainty by introducing nuisance multipliers for each and maximizing the likelihood for the agreement between prediction and data with respect to the nuisance parameters, constrained by the prior Gaussian uncertainties for each (profiling). All correlations in the systematics are maintained between signal and background. The resulting limits are presented in Table II.

In summary, we have performed a search for the standard model Higgs boson produced in association with either a Z or W boson (denoted as VH), in the final state topology requiring missing transverse momentum and two b -tagged jets in 0.93 fb^{-1} of data. In the absence of a significant excess in data above the background expectation, we set limits on $\sigma(p\bar{p} \rightarrow VH) \times B(H \rightarrow b\bar{b})$ at the 95% confidence level of 2.6–2.3 pb for Higgs boson masses in the range 105–135 GeV. The corresponding expected limits range from 2.8–2.0 pb. The expected and observed limits, along with the SM prediction, are shown in Fig. 4 as a function of Higgs mass. This is the most stringent limit to date using the missing energy and acoplanar b -jet topology at a hadron collider. The sensitivity should increase significantly in the near future with the continuing accumulation of luminosity from the Tevatron and improvement in analysis techniques.

We thank the staffs at Fermilab and collaborating institutions, and acknowledge support from the DOE and NSF (USA); CEA and CNRS/IN2P3 (France); FASI, Rosatom and RFBR (Russia); CNPq, FAPERJ, FAPESP and FUNDUNESP (Brazil); DAE and DST (India); Colciencias (Colombia); CONACyT (Mexico); KRF and KOSEF (Korea); CONICET and UBACyT (Argentina); FOM (The Netherlands); STFC (United Kingdom); MSMT and GACR (Czech Republic); CRC Program, CFI, NSERC and WestGrid Project (Canada); BMBF and DFG (Germany); SFI (Ireland); The Swedish Research

Council (Sweden); CAS and CNSF (China); and the Alexander von Humboldt Foundation (Germany).

*Visitor from Augustana College, Sioux Falls, SD, USA.

†Visitor from The University of Liverpool, Liverpool, United Kingdom.

‡Visitor from ECFM, Universidad Autonoma de Sinaloa, Culiacán, Mexico.

§Visitor from II. Physikalisches Institut, Georg-August-University, Göttingen, Germany.

||Visitor from Helsinki Institute of Physics, Helsinki, Finland.

¶Visitor from Universität Bern, Bern, Switzerland.

**Visitor from Universität Zürich, Zürich, Switzerland.

††Deceased.

- [1] G. Abbiendi *et al.* (ALEPH, DELPHI, L3, and OPAL Collaborations), Phys. Lett. B **565**, 61 (2003).
- [2] LEP Electroweak Working Group, <http://lepewwg.web.cern.ch/LEPEWWG/>.
- [3] T. Aaltonen *et al.* (CDF Collaboration), Phys. Rev. Lett. **100**, 211801 (2008).
- [4] V.M. Abazov *et al.* (D0 Collaboration), Phys. Rev. Lett. **97**, 161803 (2006).
- [5] V.M. Abazov *et al.* (D0 Collaboration), Phys. Lett. B **663**, 26 (2008).
- [6] T. Aaltonen *et al.* (CDF Collaboration), Phys. Rev. Lett. **100**, 041801 (2008).
- [7] V.M. Abazov *et al.* (D0 Collaboration), Phys. Lett. B **655**, 209 (2007).
- [8] T. Aaltonen *et al.* (CDF Collaboration), arXiv:0807.4493 [Phys. Rev. Lett. (to be published)].
- [9] V.M. Abazov *et al.* (D0 Collaboration), Nucl. Instrum. Methods Phys. Res., Sect. A **565**, 463 (2006).
- [10] T. Andeen *et al.*, Fermilab Report No. FERMILAB-TM-2365, 2007.
- [11] V.M. Abazov *et al.* (D0 Collaboration), Phys. Rev. Lett. **101**, 062001 (2008).
- [12] T. Sjöstrand *et al.*, arXiv:hep-ph/0308153, 2003. We used PYTHIA version 6.323.
- [13] M.L. Mangano *et al.*, J. High Energy Phys. 07 (2003) 001.
- [14] R. Brun and F. Carminati, CERN Program Library Long Writup Report No. W5013, 1993.
- [15] T. Scanlon, Fermilab Report No. FERMILAB-THESIS-2006-43, 2006.
- [16] T. Junk, Nucl. Instrum. Methods Phys. Res., Sect. A **434**, 435 (1999).
- [17] W. Fisher, Fermilab Report No. FERMILAB-TM-2386-E, 2007.